Fyn is a redox sensor involved in solar ultraviolet light-induced signal transduction in skin carcinogenesis

Jong-Eun Kim[1,2,3,†], **Eunmiri Roh**[1,†], **Mee Hyun Lee**[1,4], **Dong Hoon Yu**[1], **Dong Joon Kim**[1], **Tae-Gyu Lim**[1,2,3], **Sung Keun Jung**[1,2], **Cong Peng**[1], **Yong-Yeon Cho**[1,5], **Sally Dickinson**[6], **Dave Alberts**[6], **G. Tim Bowden**[6], **Janine Einspahr**[6], **Steven P Stratton**[6], **Clara Curiel**[6], **Ann M. Bode**[1], **Ki Won Lee**[2,3,*], and **Zigang Dong**[1,*]

[1]The Hormel Institute, University of Minnesota, USA

[2]WCU Major in Biomodulation, Department of Agricultural Biotechnology, Seoul National University, Seoul, Republic of Korea

[3]Advanced Institutes of Convergence Technology, Seoul National University, Suwon, Gyeonggi-do, Republic of Korea

[4]China-US Hormel Cancer Institute, Zhenzhou, Henan, China

[5]College of Pharmacy, The Catholic University of Korea, Bucheon-si, Gyeonggi-do, Republic of Korea

[6]University of Arizona Cancer Center, Tucson, AZ, USA

Abstract

Solar ultraviolet (UV) light is a major etiological factor in skin carcinogenesis, with solar UV-stimulated signal transduction inducing pathological changes and skin damage. The primary sensor of solar UV-induced cellular signaling has not been identified. We use an experimental system of solar simulated light (SSL) to mimic solar UV and we demonstrate that Fyn is a primary redox sensor involved in SSL-induced signal transduction. Reactive oxygen species (ROS) generated by SSL exposure directly oxidize Cys488 of Fyn, resulting in increased Fyn kinase activity. Fyn oxidation was increased in mouse skin after SSL exposure, and Fyn knockout ($Fyn^{-/-}$) mice formed larger and more tumors compared to Fyn wildtype mice when exposed to SSL for an extended period of time. Murine embryonic fibroblasts (MEFs) lacking Fyn as well as cells in which Fyn expression was knocked down were resistant to SSL-induced apoptosis. Furthermore, cells expressing mutant Fyn (C448A) were resistant to SSL-induced apoptosis.

Correspondence should be addressed to: Zigang Dong, The Hormel Institute, University of Minnesota, 801 16th Ave NE, Austin, MN 55912. Tel: 1-507-437-9600; FAX: 1-507-437-9606; zgdong@hi.umn.edu, Ki Won Lee, PhD: WCU Major in Biomodulation, Department of Agricultural Biotechnology, Seoul National University, Seoul, Republic of Korea,151-921, Tel:82-2-880-4661; Fax: 82-2-878-6178; kiwon@snu.ac.kr.
†These authors contributed equally to this work

These findings suggest that Fyn acts as a regulatory nexus between solar UV, ROS and signal transduction during skin carcinogenesis.

Keywords

kinase activity; reactive oxygen species; redox state; signal transduction; solar ultraviolet; solar simulated light

Introduction

Skin cancer is the most common cancer in the United States, with more cases diagnosed each year than breast, prostate, lung and colon cancers combined[35]. Solar ultraviolet (UV; i.e. sunlight) irradiation is a major etiological environmental factor in the development of skin cancers, including basal cell carcinomas (BCC), squamous cell carcinomas (SCC) and melanomas. Recent studies have shown that approximately 90% of nonmelanomas and 86% of melanoma skin cancers are associated with exposure to solar UV[1, 27, 28, 30]. The role of solar UV in skin cancer development has been the subject of intensive research efforts for many years. Solar UV activates numerous cellular signal transduction pathways leading to changes in gene expression patterns that are associated with carcinogenesis.

The Src family of protein tyrosine kinases plays crucial roles in regulating signal transduction through a number of cell surface receptors[31]. Fyn is a prominent member and is ubiquitously expressed in the human body, including the skin. Fyn comprises an N-terminal region required for plasma membrane binding, two Src homology (SH) domains (SH2 and SH3) involved in protein–protein interactions, a catalytic domain that includes an adenosine triphosphate (ATP)-binding site and a C-terminal tail containing a site that negatively regulates tyrosine phosphorylation[33]. Previous studies have focused on the relationship between solar UV and Fyn[17, 23, 37], demonstrating that solar UV induces Fyn activity. In addition, a number of cellular signals that are induced by solar UV are also mediated by Fyn[33]. However, the detailed mechanism responsible explaining how solar UV activates Fyn has not been elucidated.

When solar UV photons strike the skin, they are absorbed by the epidermal layers until the energy dissipates[18]. The absorption of solar UV irradiation occurs through chromophores such as tryptophan, urocanic acid, riboflavin and others, which are present in skin cells and generate reactive oxygen species (ROS), including hydrogen peroxide (H_2O_2), the superoxide anion radical (O^{2-}), the hydroxyl radical (OH), singlet oxygen molecules ($^1O_2$), as well as lipid peroxides, and their radicals (LOOH and LOO^-)[39]. The resultant ROS generation is a key mediator of solar UV-induced cellular signaling[14]. However, the primary activator of the downstream signaling pathways involved has remained elusive. For our studies, we use a solar simulated light (SSL) source as an experimental model to mimic solar UV. Here, we report that Fyn is an initial effector of ROS-mediated signal transduction induced by SSL. We also demonstrate the role of Fyn in SSL-induced skin carcinogenesis. Mice lacking Fyn ($Fyn^{-/-}$) developed larger and greater numbers of tumors compared to wildtype ($Fyn^{+/+}$) mice when exposed to SSL for extended time periods. Murine embryonic fibroblasts (MEFs) lacking Fyn ($Fyn^{-/-}$) and cells expressing knockdown Fyn (shFyn) were

highly resistant to SSL-induced apoptosis. Taken together, these results suggest that Fyn acts as a central regulatory nexus between solar UV exposure, ROS and signal transduction in skin carcinogenesis.

Results

SSL induces Fyn kinase activity and downstream signal transduction

Previous studies have shown that Fyn, a member of the Src family of kinases, plays an important role in signal transduction[33]. We first observed that SSL could activate Fyn kinase activity in HaCaT human and JB6 Cl41 mouse skin cells in a time- (Fig. 1A and B, respectively) and dose- (Fig. 1C and D, respectively) dependent manner. Fyn was maximally activated immediately (0 min) after exposure to 60 kJ/m^2 of SSL in HaCaT cells and at 5 min of 60 kJ/m^2 SSL irradiation in JB6 cells. Fyn signaling, including downstream JNKs and p38 that are known to be activated by SSL, was suppressed by Fyn knockout (Fyn$^{-/-}$) or Fyn silencing (shFyn) constructs, (Fig. 1 E and F, respectively). The pharmacological Fyn inhibitor, PP2, also attenuated Fyn signaling (Supplementary Fig. 1).

Fyn is activated by reactive oxygen species (ROS)

We next examined a potential role for ROS in SSL-induced signaling involving Fyn. We used the glutathione precursor, N-acetylcysteine (NAC), and an enzymatic scavenger of H_2O_2, catalase, to alter cellular redox states and found that either of these agents could attenuate SSL-induced Fyn activity (Fig. 2A and B, respectively) and its downstream signaling (Fig. 2C and D). H_2O_2 induced Fyn kinase activity in HaCaT cells (Fig. 2Ea) and mouse embryonic fibroblasts (MEFs, Fig. 2Eb) and activated JNKs, p38 and PKCδ phosphorylation in wildtype (Fyn$^{+/+}$) MEFs (Fig. 2F). However, H_2O_2 did not stimulate phosphorylation of JNKs, p38 or PKCδ in Fyn$^{-/-}$ MEFs (Fig. 2F). Collectively, these results suggest that Fyn plays a key role in SSL-induced signaling that is mediated by ROS, such as H_2O_2.

Cysteine 488 is a key residue in the activation of Fyn by SSL mediated by ROS

To determine whether ROS (such as H_2O_2) can activate Fyn directly, we constructed a cysteine mutant, cysteine-488-alanine (C488A). C488A was selected on the basis of its importance in terms of corresponding residues in another Src family kinase, Lyn, which is responsive to ROS[41]. We then transfected a wildtype Fyn or mutant Fyn C488A plasmid into 293T cells. Wildtype (wt) Fyn and Fyn mutant (C488A) proteins were immunoprecipitated and treated with H_2O_2 (15 μM). Results showed that H_2O_2 treatment resulted in tyrosine phosphorylation of the wt Fyn target, PKCδ, but had less effect on PKCδ in the mutant Fyn C488A (Fig. 3A). SSL had similar effects on PKCδ in wildtype compared to mutant Fyn (Fig. 3B). We then assessed reduced and oxidized Fyn cysteine residues using biotinylated iodoacetamide (BIAM) labeling for reduction and iodoacetic acid (IAA) and BIAM carboxymethylation double-labeling to assess oxidation, respectively[12]. We found that the C488A mutant-expressing cells exhibited substantially less oxidation compared to the Fyn wt-expressing cells (Fig. 3C). To verify that Fyn undergoes oxidation when subjected to SSL *in vivo*, SKH-1 hairless mice were exposed to H_2O_2 (as a control) or SSL irradiation and then skin proteins were recovered at the indicated time points. The redox status of Fyn was

measured using the same method as for the *in vitro* experiments. Fyn oxidation increased whereas Fyn reduction decreased in mouse skin exposed to either H_2O_2 or SSL *in vivo* (Fig. 3D). H_2O_2 or SSL-induced phosphorylation of JNKs, p38 and PKCδ, which are downstream of Fyn (Fig. 3E). SSL-induced phosphorylation of JNKs, p38 and PKCδ was also decreased in C488A mutant Fyn MEFs (Fig. 3F), C488A HaCaT (Fig. 3G) or C488A HeLa (Fig. 3H) cells compared to the respective cells overexpressing wt Fyn.

Fyn-knockout (Fyn$^{-/-}$) SKH-1 hairless mice develop larger and greater numbers of tumors when exposed to SSL

To further investigate the role of Fyn in SSL-induced skin carcinogenesis, we exposed Fyn$^{-/-}$ and Fyn$^{+/+}$ SKH-1 hairless mice to SSL for 12 weeks. Treatment was then stopped and tumor growth was observed for an additional 13 weeks. Tumors began to emerge at Week 17; however, the Fyn$^{+/+}$ mice exhibited fewer and smaller tumors compared to their Fyn$^{-/-}$ counterparts (Fig. 4 A–D). The size (mm^3) of tumors in SSL-treated mouse skin was significantly greater in Fyn$^{-/-}$ SKH-1 mice ($p < 0.01$; Fig. 4C) and the average number of SSL-induced tumors per mouse was also significantly increased in Fyn$^{-/-}$ SKH-1 mice compared with Fyn$^{+/+}$ mice ($p < 0.01$; Fig. 4D). In addition, SSL treatment increased epidermal thickness associated with edema and epithelial cell proliferation (Fig. 4B). H&E staining revealed that after treatment with SSL, epidermal thicknesses in Fyn$^{+/+}$ SKH-1 mice were increased compared to untreated mice, an observation that supports the findings of previous studies[22, 29]. However, Fyn$^{-/-}$ SKH-1 mice showed a much greater increase in epidermal thickness compared to Fyn$^{+/+}$ mice (Fig. 4B). These results demonstrate that lack of Fyn increases SSL-induced tumor formation.

Fyn deficiency confers resistance against SSL-induced apoptosis

Fyn$^{-/-}$ MEFs were less responsive to SSL-induced apoptosis compared to Fyn$^{+/+}$ MEFs (Fig. 5A, Supplementary Fig. 2A). HaCaT cells expressing shFyn were also less responsive to SSL-induced apoptosis compared to mock-expressing cells (Fig. 5B, Supplementary Fig. 2B). SSL-induced pro-apoptotic signaling through cleavage of caspase-3, caspase-9 or PARP was reduced in Fyn$^{-/-}$ SKH-1 mice (Fig. 5C), in cells deficient in Fyn (Fig. 5D) or in cells deficient in Fyn (Fig. 5E). Fyn is known to regulate both pro-apoptotic signaling (e.g., JNKs, p38 and PKCδ) and anti-apoptotic signaling (e.g., ERKs and Akt). SSL-induced apoptosis decreased with Fyn deficiency, implying that SSL-induced Fyn activation increases pro-apoptotic signaling to a greater extent than anti-apoptotic signaling, which could indicate that Fyn is required for SSL-induced apoptosis to prevent skin carcinogenesis. We also observed that treatment with the antioxidant NAC or catalase inhibited SSL-induced apoptosis (Supplementary Fig. 2C), suggesting that ROS are involved in SSL-induced apoptosis. To examine the importance of the Fyn Cys488 site for SSL-induced apoptosis, we transduced wt or mutant Fyn C488A into Fyn$^{-/-}$ MEFs or HaCaT cells. Cells were exposed to SSL and apoptosis was measured. Fyn C488A-transduced Fyn$^{-/-}$ MEFs (Fig. 5F) or HaCaT cells (Fig. 5G) were more resistant to apoptosis compared to their respective wildtype counterparts. These results demonstrate that Cys488 is necessary for SSL-induced apoptosis.

Fyn phosphorylates PKCδ to mediate SSL-induced apoptosis

Tyrosine phosphorylation of PKC correlates with UV induced apoptosis[11] and Fyn phosphorylates PKCδ[16]. SSL-induced PKCδ activity was decreased by Fyn knockout in MEFs (Fig. 6A) or Fyn knockdown in HaCaT cells (Fig. 6B). SSL-induced tyrosine phosphorylation of PKCδ (Tyr313) and autophosphorylation (Ser643) were also decreased in Fyn knockout mouse skin (Fig. 6C) and in MEFs (Fig. 6D) as well as by knockdown of Fyn in HaCaT cells (Fig. 6E. Phosphorylation of PKCδ (Thr505) was also decreased in Fyn$^{-/-}$ MEFs or shPKCδ HaCaT cells (Fig. 6D, E). We could not detect Ser643 of PKCδ *in vivo*. Knockdown PKCδ using shRNA decreased apoptosis (Fig. 6F, Supplementary Fig. 2D) and apoptotic signaling (Fig 6G and H), to a similar extent observed in Fyn knockdown cells except for JNKs signaling. These results demonstrate that the PKCδ/p38 pathway is one of the mediators of SSL-induced apoptosis that involves Fyn activation.

Discussion

Solar UV is a major etiological environmental factor in skin cancer and aging, and comprises approximately 95% UVA and 5% UVB irradiation. Both UVA and UVB can activate signal transduction pathways related to inflammation and apoptosis, and under normal sunlight conditions, both types irradiate the skin. The identification of the cellular signaling pathway(s) induced by solar UV and their roles in skin carcinogenesis need to be fully understood in order to support the development of novel therapeutics to treat malignant skin cells. We used UV-340 lamps to mimic solar UV and irradiated HaCaT cells, MEFs and a hairless mouse model. We observed that solar simulated light (SSL; 60 kJ UVA/m^2, 3.6 kJ UVB/m^2), which is equivalent to 15 minutes of sun exposure in Austin, Minnesota, in midsummer from 2 to 4 p.m., could activate Fyn[25].

Cellular chromophores such as aromatic amino acids, porphyrins, urocanic acid, and DNA can convert irradiation energy into chemical energy[19]. ROS molecules activate a number of cellular signaling pathways[5, 40]. However, a direct connection between solar UV-induced ROS and solar UV-induced signal transduction has not previously been identified. In this study, we provide evidence showing that Fyn is a critical link between ROS and cellular signal transduction, which suggests a prominent role for Fyn in solar UV-induced skin carcinogenesis. Solar UV increases the generation of ROS, resulting in the activation of Fyn and subsequent downstream cellular signaling pathways. ROS are known to modulate downstream pathways by reacting with specific protein targets through the oxidative modification of key cysteine residues. Src family kinases such as c-Src and Lyn are also activated by oxidative modification[41]. Using homology studies between c-Src, Lyn, and Fyn, we identified Cys488 as a key Fyn residue undergoing oxidative modification[41]. c-Src contains Cys487, which is a homological residue to Fyn Cys488, and is also important in H_2O_2-induced c-Src kinase activation[13]. Cys488 is located in the kinase domain of the Fyn protein and a conservative mutation of the cysteine to alanine gives rise to a redox-insensitive kinase, which cannot be fully activated. Mounting evidence describes Fyn activation through its redox regulation as a key mediator in solar UV-induced skin carcinogenesis.

Src family kinases have frequently been regarded as oncogenes[2], with Fyn reportedly promoting many types of cancer[33]. The overexpression of constitutively active Fyn in skin causes the spontaneous formation of tumors[42]. We previously reported that Src family kinase inhibitors, including myricetin and apigenin, inhibited UV-induced skin carcinogenesis[7, 8, 20, 21, 29, 34]. However, in our SSL-exposed skin cancer model, our results demonstrated that Fyn$^{-/-}$ SKH-1 mice developed larger and greater numbers of tumors compared to Fyn$^{+/+}$ SKH-1 mice. This suggests that Fyn activation by SSL suppresses tumor formation, revealing a novel aspect of Fyn. Some kinases are known to function both as oncogenes and tumor suppressors. During low-level activation of some kinases, inflammation can occur, with chronic inflammation promoting tumor growth. However, high-level activation of such kinases can stimulate signaling pathways that induce cell death[36]. The p38 protein is one such example and acts as a major mediator of diverse inflammatory and apoptotic signaling pathways that are dependent on the nature of its induction and the tissue type[26]. In this study, we show a new perspective on Fyn as an apoptotic mediator with similarities to the p38 MAPK.

The skin protects the body from physical damage, microbial infection and dehydration. Damaged skin cells that cannot be repaired must be efficiently removed to maintain normal function, but an incorrect balance of apoptosis (cell death) and proliferation is associated with many types of skin disease[32]. The balance between the pro-apoptotic and anti-apoptotic signaling cascades determines cell fate decisions and must remain fine-tuned for optimal skin health[24]. Contradictory evidence exists as to whether Fyn is up- or down-regulated during apoptosis[10, 37, 38]. PKCδ is a well-studied regulator of cell death and survival in solar UV-damaged skin cells[3], and previous studies have shown that Fyn can phosphorylate PKCδ. The role of tyrosine phosphorylation of PKCδ by Fyn in PKCδ activity remains controversial[3, 4, 6, 15]. In our study, both knockdown and knockout of Fyn reduced SSL-induced tyrosine phosphorylation and PKCδ activity. Changes in SSL-induced signal transduction in PKCδ knockdown cells were similar for that of Fyn. SSL appears to induce the activation of PKCδ activity through tyrosine phosphorylation by Fyn. These results suggest that the ROS/Fyn/PKCδ axis plays a major role in solar UV-induced cell signal transduction and regulation of apoptosis in the skin.

We report that Fyn is a critical initial point of signal transduction induced by SSL and acts as a redox sensor in SSL-induced signal transduction. ROS directly activate Fyn kinase activity through the oxidation of the Fyn Cys488 residue. Fyn subsequently activates downstream signaling, including JNKs, p38 and PKCδ, which are effectors that play critical roles in stimulating apoptosis. In addition, Fyn$^{-/-}$ SKH-1 mice were more resistant to SSL-induced apoptosis and therefore more susceptible to SSL-induced carcinogenesis compared to their Fyn$^{+/+}$ counterparts.

Materials and Methods

Reagents

Active Fyn, PP2, catalase, NAC were purchased from Merck Millipore (Billerica, MA). The Src substrate peptide (KVEKIGEGTYGVVYK) was purchased from SignalChem (Richmond, Canada). Antibodies specific to detect total MKK3/6, phosphorylated MKK3/6

(Ser189/207), total p38, phosphorylated p38 (Thr180/Tyr182), total MKK4, phosphorylated MKK4 (Ser257/Thr261), total JNKs, phosphorylated JNKs (Ser112), total c-Jun, phosphorylated c-Jun (Ser73), total PKCδ, phosphorylated PKCδ (Y313, T505 and S643), PARP, caspase-3, and caspase-9 were purchased from Cell Signaling Technology (Beverly, MA). Antibodies to detect total Fyn, total MSK, phosphorylated MSK1 (Ser376) and β-actin were purchased from Santa Cruz Biotechnology (Santa Cruz, CA).

Cell culture

$Fyn^{+/+}$ and $Fyn^{-/-}$ MEFs were isolated from $Fyn^{+/+}$ SKH-1 and $Fyn^{-/-}$ SKH-1 hairless mice and cultured as described[9]. All cell lines were purchased from the American Type Culture Collection and were cytogenetically tested and authenticated before being frozen. Each vial of frozen cells was thawed and maintained in culture for a maximum of 8 weeks. Enough frozen vials were available for each cell line to ensure that all cell-based experiments were conducted on cells that had been tested and in culture for 8 weeks or less. HaCaT skin keratinocytes were cultured in DMEM (Thermo Fisher Scientific, Inc.) supplemented with 10% FBS and 1% antibiotic–antimycotic. JB6 P+ mouse skin epidermal cells were cultured in Minimum Essential Medium supplemented with 5% FBS and 1% antibiotic–antimycotic.

SSL irradiation system

The SSL source was comprised of UVA-340 lamps purchased from Q-Lab Corporation (Westlake, OH). The UVA-340 lamps provide the best possible simulation of sunlight in the critical short wavelength region from 365 nm down to the solar cutoff of 295 nm with a peak emission of 340 nm. The percentage of UVA and UVB emitted from the UVA-340 lamps was measured by a UV meter at 94.5% and 5.5%, respectively[22] and about 30 min is required to reach a SSL dose of 60 kJ/m^2. Once the dose is reached, cells or skin samples were harvested either immediately (0 min) or as indicated thereafter.

SSL-induced skin carcinogenesis

Skin carcinogenesis in mice was induced using an experimental SSL-irradiation system. $Fyn^{+/+}$ SKH-1 and $Fyn^{-/-}$ SKH-1 hairless mice were bred, propagated, and maintained at The Hormel Institute, University of Minnesota (Austin, MN). Mice were maintained under conditions based on the guidelines established by the Research Animal Resources and the University of Minnesota Institutional Animal Care and Use Committee. The mice were divided into 4 groups of 6-wks-old mice with an average body weight of 25 g. The groups were as follows: group 1 was $Fyn^{+/+}$ (n = 8) not exposed to SSL as control; group 2 was $Fyn^{+/+}$ (n=15) exposed to SSL; group 3 was $Fyn^{-/-}$ (n = 5) not exposed to SSL as control; group 4 was $Fyn^{-/-}$ (n = 8) exposed to SSL. For the experimental SSL-treated groups, mice were initially treated with a SSL dose of 30 kJ UVA/m^2–1.8 kJ UVB/m^2 twice weekly. The dose was increased by 10% each week until week 6. At week 6, the dose reached 48 kJ UVA/m^2–2.9 kJ UVB/m^2, and this dose was maintained from week 6 to week 12. At 12 weeks, SSL exposure was discontinued, and tumor growth was monitored for an additional 13 wks. A tumor was defined as an outgrowth of > 1 mm in diameter that persisted for 2 or more weeks. Tumor numbers and volumes were recorded every week until the end of the experiment. Half of the tumor and skin samples were immediately fixed in 10% neutral-

buffered formalin (NBF) and processed for hematoxylin and eosin (H&E) staining. The other half was frozen for Western blot analysis.

Immunoblot analysis

Cell lysates were prepared with radio-immunoprecipitation assay (RIPA) buffer (50 mM Tris–HCl pH 7.4, 1% NP-40, 0.25% sodium deoxycholate, 0.1% sodium dodecyl sulfate, 150 mM NaCl, 1 mM ethylenediaminetetraacetic acid, and 1× protease inhibitor tablet). Equal loading of protein was confirmed using a bicinchoninic acid assay (Pierce, Rockford, IL). Proteins were separated by sodium dodecyl sulfate–polyacrylamide gel electrophoresis (SDS-PAGE) and transferred to polyvinylidene difluoride (PVDF) membranes (EMD Millipore). Membranes were blocked with 5% non-fat dry milk for 1 h at room temperature (RT) and incubated with the appropriate primary antibodies overnight at 4°C. After washing with phosphate-buffered saline containing 0.1% Tween 20, the membrane was incubated with a horseradish peroxidase (HRP)-conjugated secondary antibody at a 1:5000 dilution and the signal was detected with a chemiluminescence reagent (GE Healthcare, Piscataway, NJ).

Apoptosis analysis

SSL-induced apoptosis was determined using the annexin V-FITC apoptosis detection kit (MBL International Corp., Woburn, MA) following the manufacturer's instructions. After SSL irradiation, cells were harvested at the indicated time points, washed with phosphate-buffered saline, and then incubated for 5 min at room temperature with annexin V-FITC plus propidium iodide. Apoptosis was analyzed using a FACSCalibur flow cytometer (BD Biosciences, San Jose, CA)

DNA fragmentation

Cells were disrupted by adding lysis buffer (10 mM Tris-HCl, pH 8.0, 10 mM EDTA, 0.5% Triton X 100) and incubated on ice for 45–90 min followed by centrifugation at 12,000 × g for 45 min at 4°C. The supernatant fraction containing fragmented DNA was mixed with 5 μl of protease K at 50°C for 3 h and centrifuged at 12,000 × g for 30 min at 4°C. The DNA was extracted twice with phenol:chloroform:isopropyl alcohol (25:24:1) and once by chloroform. One-tenth volume of 3 M NaAc and 2 volumes of ethanol were added to the DNA extraction part and kept at −20°C for 1–2 h or overnight before centrifugation at 12,000 × g for 30 min at 4°C. The DNA pellet was washed with 70% ethanol and resuspended in Tris-EDTA buffer with 1 mg/ml RNase A. DNA fragments were separated by 2% agarose gel electrophoresis, stained with ethidium bromide, and photographed under UV light.

Fyn kinase assay

The *in vitro* kinase assays were performed following the instructions provided by Merck Millipore. In brief, every reaction solution contained 20 μL of assay dilution buffer [20 mM MOPS (pH 7.2), 25 mM β-glycerol phosphate, 5 mM EGTA, 1 mM sodium orthovanadate, and 1 mM DTT] and a magnesium-ATP cocktail buffer. For Fyn, 250 μM Src substrate peptide was also included. A 2.5-μL aliquot was removed from the reaction mixture, which

contained 2.5 μL of 250 μM Src substrate and 10 μL diluted [γ-^{32}P] ATP solution and incubated at 30°C for 30 min. Then 15-μL aliquots were transferred onto p81 paper and washed 3 times with 0.75% phosphoric acid for 5 min/wash and once with acetone for 5 min. The radioactive incorporation was determined using a scintillation counter.

For *ex vivo* Fyn immunoprecipitation and kinase assays, 500 μg of cell lysate protein was mixed with Protein A/G PLUS-Agarose beads (Santa Cruz Biotechnology, 20 μL) for 1 h at 4°C in advance. The mixture was centrifuged at 12,000 rpm for 5 min at 4°C, and a Fyn antibody (10 μg) was added to the supernatant fraction and gently rocked overnight at 4°C. These tubes were centrifuged, and pellets washed twice. The pellets were suspended in 6.5 μL of kinase buffer supplemented with 10 μL of diluted [γ-^{32}P] ATP solution and 2.5 μL of Src substrate peptide (250 μM) and incubated for 15 min at 30°C. Then 15-μL aliquots were transferred onto p81 paper and washed 3 times with 0.75% phosphoric acid for 5 min/wash and once with acetone for 5 min. The radioactive incorporation was determined using a scintillation counter.

For measuring transfected Fyn kinase activity, 500 μg of cell lysate protein was mixed with Protein A/G PLUS-Agarose beads (20 μL) for 1 h at 4°C in advance. The mixture was centrifuged at 12,000 rpm for 5 min at 4°C, and a His antibody (1 μg) was added to the supernatant fraction and gently rocked overnight at 4°C. The beads were incubated with 0.5 μg PKCδ and 100 μM of ATP for the indicated time with continuous mixing. Kinase activity was measured by Western blot using a phosphotyrosine antibody (Santa Cruz Biotechnology).

PKCδ kinase assay

The *in vitro* kinase assays for PKCδ were performed following the instructions provided by Merck Millipore. In brief, every reaction solution contained 20 μL of assay dilution buffer [20 mM MOPS (pH 7.2), 25 mM β-glycerol phosphate, 5 mM EGTA, 1 mM sodium orthovanadate, and 1 mM DTT] and a magnesium-ATP cocktail buffer. For PKCδ, 250 μM of the PKC substrate peptide (KRREILSRRPSYR) were also included. A 2.5-μL aliquot was removed from the reaction mixture, which contained 2.5 μL of 250 μM PKC substrate and 10 μL diluted [γ-^{32}P] ATP solution and incubated at 30°C for 30 min. Then 15-μL aliquots were transferred onto p81 paper and washed 3 times with 0.75% phosphoric acid for 5 min/wash and once with acetone for 5 min. The radioactive incorporation was determined using a scintillation counter.

For *ex vivo* PKCδ immunoprecipitation and kinase assays, 500 μg of cell lysate protein were mixed with Protein A/G PLUS-Agarose beads (Santa Cruz Biotechnology, 20 μL) for 1 h at 4°C in advance. The mixture was centrifuged at 12,000 rpm for 5 min at 4°C, and a PKCδ antibody (10 μg) was added to the supernatant fraction and gently rocked overnight at 4°C. These tubes were centrifuged, and pellets washed twice. The pellets were suspended in 6.5 μL of kinase buffer supplemented with 10 μL of diluted [γ-^{32}P] ATP solution and 2.5 μL of PKC substrate peptide (250 μM) and incubated for 15 min at 30°C. 15-μL aliquots were then transferred onto p81 paper and washed 3 times with 0.75% phosphoric acid for 5 min/wash and once with acetone for 5 min. The radioactive incorporation was determined using a scintillation counter.

BIAM-mediated carboxymethylation

At 24 h after transfection with pcDNA4His-Fyn, HEK293T cells were disrupted using lysis buffer [10 mM Tris (pH 7.5), 150 mM NaCl, 5 mM EDTA, 1% Triton X-100, 1 mM dithiothreitol (DTT), 0.1 mM phenylmethylsulfonyl fluoride (PMSF), 10% glycerol, and a protease inhibitor cocktail tablet] containing 100 μM BIAM (Invitrogen). Fyn was immunoprecipitated with anti-His and Protein A/G PLUS-Agarose beads (Santa Cruz Biotechnology). The immunocomplexes were separated by SDS–PAGE and BIAM labels were detected with HRP-conjugated streptavidin and ECL[41].

IAA and BIAM-mediated double carboxymethylation

For double carboxymethylation with IAA and BIAM labeling, HEK293T cells were treated as described above, with the exception that the lysis buffer contained 30 mM IAA instead of BIAM and the incubation occurred for 15 min at 37°C. Cells were treated as described above, and Fyn was immunoprecipitated with anti-His. After washing, the immunoprecipitated Fyn proteins were denatured with the addition of 200 μl lysis buffer containing 8 M urea and 30 mM IAA, and incubated for 15 min at 37°C to ensure the carboxymethylation of non-exposed reduced cysteines. Proteins were precipitated with cold acetone/HCl/H$_2$O (at a ratio of 92:2:10) to remove IAA. After centrifugation, the pellets were suspended in 50 μl lysis buffer containing 8 M urea. Thereafter, 3.5 mM DDT was added to half of each sample, and the second carboxymethylation with biotinylated probe (10 mM BIAM in lysis buffer for 15 min at 37°C) was performed to detect previously oxidized cysteines. Immunocomplexes labeled with BIAM were detected with HRP-conjugated streptavidin and ECL[12].

Statistical analysis

All quantitative results are expressed as mean values ± S.D. or S.E. as indicated. Statistically significant differences were determined using the Student t test or by one-way ANOVA. Values of $p < 0.05$ were considered to be statistically significant.

Supplementary Material

Refer to Web version on PubMed Central for supplementary material.

Acknowledgements

References

1. Abdel-Malek ZA, Kadekaro AL, Swope VB. Stepping up melanocytes to the challenge of UV exposure. Pigment Cell and Melanoma Research. 2010; 23:171–186. [PubMed: 20128873]

2. Aleshin A, Finn RS. SRC: A century of science brought to the clinic. Neoplasia. 2010; 12:599–607. [PubMed: 20689754]

3. Basu A, Pal D. Two faces of protein kinase Cdelta: the contrasting roles of PKCdelta in cell survival and cell death. The Scientific World Journal. 2010; 10:2272–2284. [PubMed: 21103796]

4. Benes C, Soltoff SP. Modulation of PKCdelta tyrosine phosphorylation and activity in salivary and PC-12 cells by Src kinases. American journal of physiology Cell physiology. 2001; 280:C1498–C1510. [PubMed: 11350745]

5. Bickers DR, Athar M. Oxidative stress in the pathogenesis of skin disease. J Invest Dermatol. 2006; 126:2565–2575. [PubMed: 17108903]

6. Breitkreutz D, Braiman-Wiksman L, Daum N, Denning MF, Tennenbaum T. Protein kinase C family: on the crossroads of cell signaling in skin and tumor epithelium. Journal of cancer research and clinical oncology. 2007; 133:793–808. [PubMed: 17661083]

7. Byun S, Lee KW, Jung SK, Lee EJ, Hwang MK, Lim SH, et al. Luteolin inhibits protein kinase C(epsilon) and c-Src activities and UVB-induced skin cancer. Cancer Res. 2010; 70:2415–2423. [PubMed: 20215519]

8. Byun S, Park J, Lee E, Lim S, Yu JG, Lee SJ, et al. Src kinase is a direct target of apigenin against UVB-induced skin inflammation. Carcinogenesis. 2013; 34:397–405. [PubMed: 23161610]

9. Chan CB, Liu X, Jung DY, Jun JY, Luo HR, Kim JK, et al. Deficiency of phosphoinositide 3-kinase enhancer protects mice from diet-induced obesity and insulin resistance. Diabetes. 2010; 59:883–893. [PubMed: 20068140]

10. Chen ZY, Cai L, Zhu J, Chen M, Chen J, Li ZH, et al. Fyn requires HnRNPA2B1 and Sam68 to synergistically regulate apoptosis in pancreatic cancer. Carcinogenesis. 2011; 32:1419–1426. [PubMed: 21642356]

11. Fukunaga M, Oka M, Ichihashi M, Yamamoto T, Matsuzaki H, Kikkawa U. UV-induced tyrosine phosphorylation of PKC delta and promotion of apoptosis in the HaCaT cell line. Biochem Biophys Res Commun. 2001; 289:573–579. [PubMed: 11716513]

12. Giannoni E, Buricchi F, Raugei G, Ramponi G, Chiarugi P. Intracellular reactive oxygen species activate Src tyrosine kinase during cell adhesion and anchorage-dependent cell growth. Mol Cell Biol. 2005; 25:6391–6403. [PubMed: 16024778]

13. Giannoni E, Taddei ML, Chiarugi P. Src redox regulation: again in the front line. Free radical biology & medicine. 2010; 49:516–527. [PubMed: 20434540]

14. Hanson KM, Clegg RM. Observation and quantification of ultraviolet-induced reactive oxygen species in ex vivo human skin. Photochemistry and photobiology. 2002; 76:57–63. [PubMed: 12126308]

15. Humphries MJ, Ohm AM, Schaack J, Adwan TS, Reyland ME. Tyrosine phosphorylation regulates nuclear translocation of PKCdelta. Oncogene. 2008; 27:3045–3053. [PubMed: 18059334]

16. Joseloff E, Cataisson C, Aamodt H, Ocheni H, Blumberg P, Kraker AJ, et al. Src family kinases phosphorylate protein kinase C delta on tyrosine residues and modify the neoplastic phenotype of skin keratinocytes. J Biol Chem. 2002; 277:12318–12323. [PubMed: 11812791]

17. Jung SK, Lee KW, Byun S, Kang NJ, Lim SH, Heo YS, et al. Myricetin suppresses UVB-induced skin cancer by targeting Fyn. Cancer Res. 2008; 68:6021–6029. [PubMed: 18632659]

18. Krutmann, J. Pathomechanisms of Photoaged Skin. In: Farage, M.; Miller, K.; Maibach, H., editors. Textbook of Aging Skin. Berlin Heidelberg: Springer; 2010. p. 101-107.

19. Kulms D, Schwarz T. 20 years after--milestones in molecular photobiology. The journal of investigative dermatology Symposium proceedings / the Society for Investigative Dermatology, Inc [and] European Society for Dermatological Research. 2002; 7:46–50.

20. Lee KM, Lee KW, Byun S, Jung SK, Seo SK, Heo YS, et al. 5-deoxykaempferol plays a potential therapeutic role by targeting multiple signaling pathways in skin cancer. Cancer prevention research. 2010; 3:454–465. [PubMed: 20233901]

21. Lee KM, Lee KW, Jung SK, Lee EJ, Heo YS, Bode AM, et al. Kaempferol inhibits UVB-induced COX-2 expression by suppressing Src kinase activity. Biochem Pharmacol. 2010; 80:2042–2049. [PubMed: 20599768]

22. Li J, Malakhova M, Mottamal M, Reddy K, Kurinov I, Carper A, et al. Norathyriol suppresses skin cancers induced by solar ultraviolet radiation by targeting ERK kinases. Cancer Res. 2012; 72:260–270. [PubMed: 22084399]

23. Li W, Marshall C, Mei L, Gelfand J, Seykora JT. Srcasm corrects Fyn-induced epidermal hyperplasia by kinase down-regulation. J Biol Chem. 2007; 282:1161–1169. [PubMed: 17046829]

24. Lippens S, Hoste E, Vandenabeele P, Agostinis P, Declercq W. Cell death in the skin. Apoptosis. 2009; 14:549–569. [PubMed: 19221876]

25. Liu K, Yu D, Cho YY, Bode AM, Ma W, Yao K, et al. Sunlight UV-induced skin cancer relies upon activation of the p38alpha signaling pathway. Cancer Res. 2013; 73:2181–2188. [PubMed: 23382047]

26. Loesch M, Chen G. The p38 MAPK stress pathway as a tumor suppressor or more? Frontiers in bioscience : a journal and virtual library. 2008; 13:3581–3593. [PubMed: 18508457]

27. Madan V, Lear JT, Szeimies RM. Non-melanoma skin cancer. The Lancet. 2010; 375:673–685.

28. Narayanan DL, Saladi RN, Fox JL. Ultraviolet radiation and skin cancer. International Journal of Dermatology. 2010; 49:978–986. [PubMed: 20883261]

29. Oi N, Chen H, Ok Kim M, Lubet RA, Bode AM, Dong Z. Taxifolin suppresses UV-induced skin carcinogenesis by targeting EGFR and PI3K. Cancer Prev Res (Phila). 2012; 5:1103–1114. [PubMed: 22805054]

30. Parkin DM, Mesher D, Sasieni P. 13. Cancers attributable to solar (ultraviolet) radiation exposure in the UK in 2010. British journal of cancer. 2011; 105(Suppl 2):S66–S69. [PubMed: 22158324]

31. Parsons SJ, Parsons JT. Src family kinases, key regulators of signal transduction. Oncogene. 2004; 23:7906–7909. [PubMed: 15489908]

32. Raj D, Brash DE, Grossman D. Keratinocyte apoptosis in epidermal development and disease. J Invest Dermatol. 2006; 126:243–257. [PubMed: 16418733]

33. Saito YD, Jensen AR, Salgia R, Posadas EM. Fyn: a novel molecular target in cancer. Cancer. 2010; 116:1629–1637. [PubMed: 20151426]

34. Shim JH, Su ZY, Chae JI, Kim DJ, Zhu F, Ma WY, et al. Epigallocatechin gallate suppresses lung cancer cell growth through Ras-GTPase-activating protein SH3 domain-binding protein 1. Cancer Prev Res (Phila). 2010; 3:670–679. [PubMed: 20424128]

35. Siegel R, Naishadham D, Jemal A. Cancer statistics, 2013. CA: A Cancer Journal for Clinicians. 2013; 63:11–30. [PubMed: 23335087]

36. Sui X, Kong N, Ye L, Han W, Zhou J, Zhang Q, et al. p38 and JNK MAPK pathways control the balance of apoptosis and autophagy in response to chemotherapeutic agents. Cancer letters. 2014; 344:174–179. [PubMed: 24333738]

37. Tang X, Feng Y, Ye K. Src-family tyrosine kinase fyn phosphorylates phosphatidylinositol 3-kinase enhancer-activating Akt, preventing its apoptotic cleavage and promoting cell survival. Cell Death Differ. 2007; 14:368–377. [PubMed: 16841086]

38. Vasant C, Rajaram R, Ramasami T. Apoptosis of lymphocytes induced by chromium(VI/V) is through ROS-mediated activation of Src-family kinases and caspase-3. Free Radical Biology and Medicine. 2003; 35:1082–1100. [PubMed: 14572611]

39. Wagener FA, Carels CE, Lundvig DM. Targeting the redox balance in inflammatory skin conditions. International journal of molecular sciences. 2013; 14:9126–9167. [PubMed: 23624605]

40. Xu Y, Fisher GJ. Ultraviolet (UV) light irradiation induced signal transduction in skin photoaging. Journal of Dermatological Science Supplement. 2005; 1:S1–S8.

41. Yoo SK, Starnes TW, Deng Q, Huttenlocher A. Lyn is a redox sensor that mediates leukocyte wound attraction in vivo. Nature. 2011; 480:U109–U278.

42. Zhao L, Li W, Marshall C, Griffin T, Hanson M, Hick R, et al. Srcasm inhibits Fyn-induced cutaneous carcinogenesis with modulation of Notch 1 and p53. Cancer research. 2009; 69:9439–9447. [PubMed: 19934324]
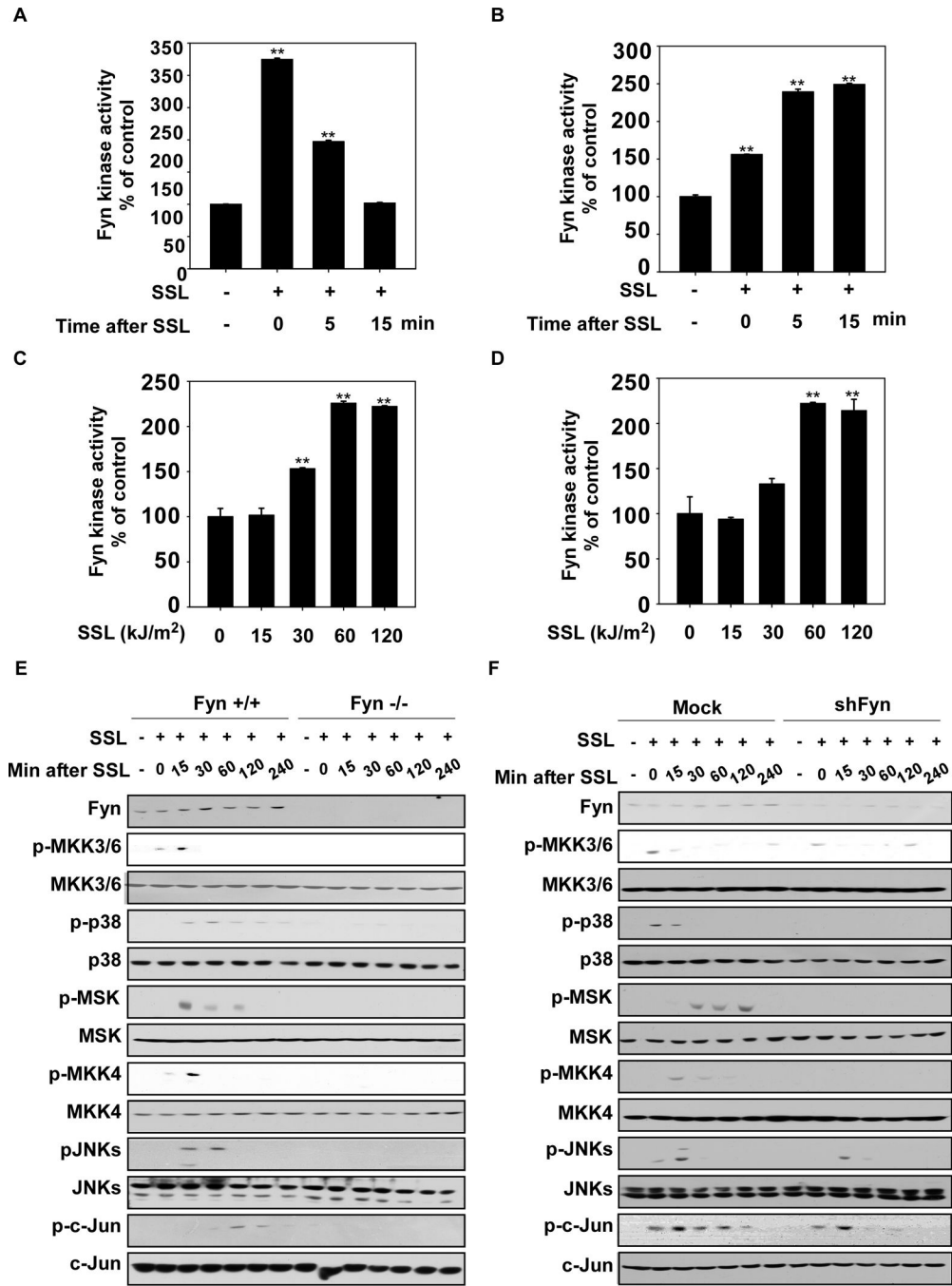
Figure 1.
Fyn is activated by SSL exposure. HaCaT (A) or JB6 Cl41 (B) cells were exposed to solar simulated light (SSL, 60 kJ/m^2) and Fyn kinase activity was measured at various time points after SSL as indicated (0 = immediately after SSL; 5 or 15 min after SSL). (C) HaCaT cells were (15, 30, 60, 120 kJ/m^2) or were not (0) exposed to SSL as indicated and kinase activity was measured immediately after exposure. (D) JB6 Cl41 cells were exposed to SSL as indicated and kinase activity was measured at 5 min after exposure. (E) Wildtype Fyn (Fyn$^{+/+}$) and Fyn-deficient (Fyn$^{-/-}$) mouse embryonic fibroblasts (MEFs) and (F) Mock-

and shFyn-expressing HaCaT cells were irradiated with SSL (60 kJ/m^2) and harvested at various time points after SSL exposure as indicated. Western blot analysis was performed and representative blots are shown. For A–D, data are represented as means ± S.D. from triplicate experiments. The asterisks (**) indicate a significant difference ($p < 0.01$) compared to the untreated control. Fyn kinase activity was measured as described in Materials and Methods.
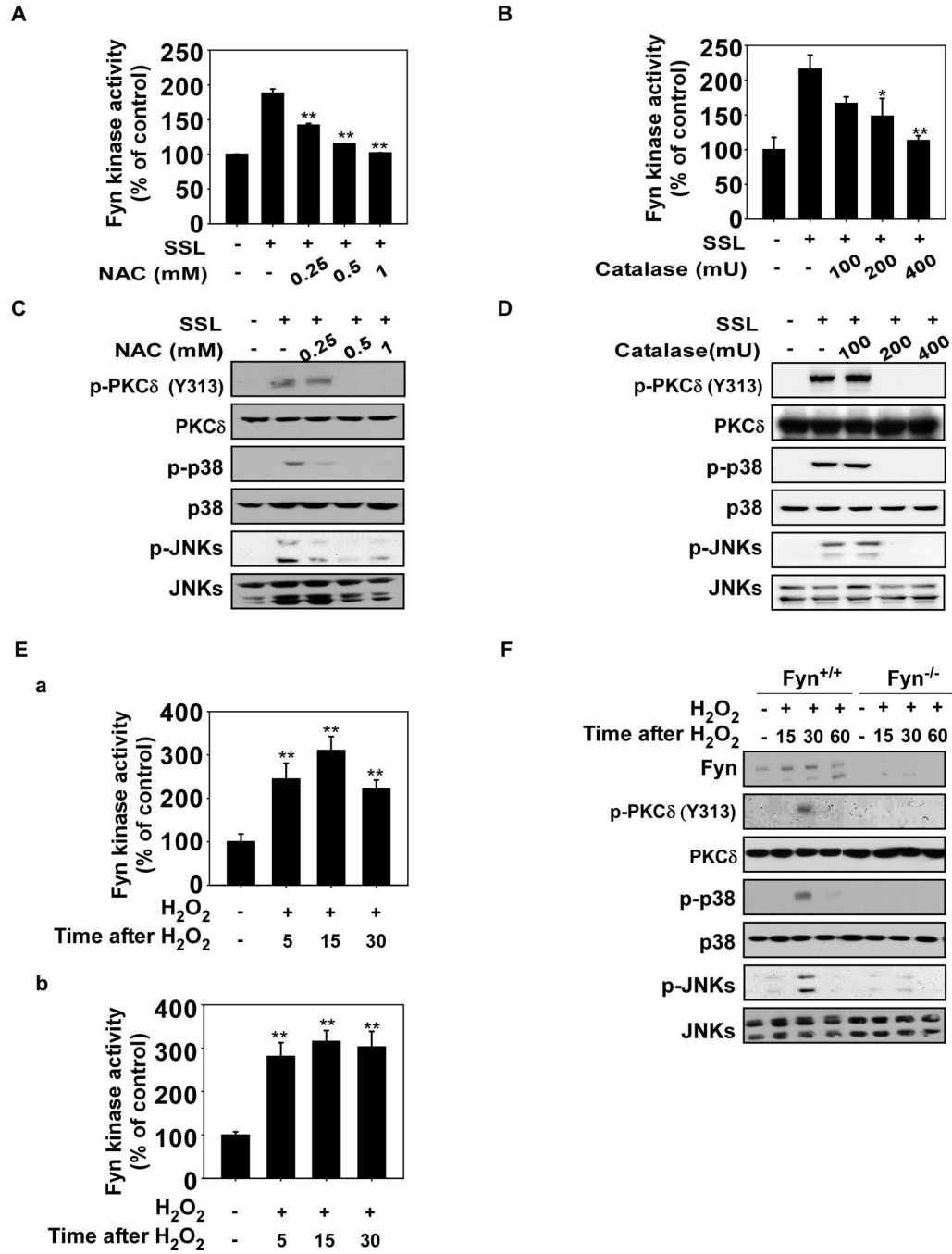
Figure 2.
Reactive oxygen species (ROS) mediate SSL-induced Fyn kinase activation. (A) N-acetylcysteine (NAC) or (B) catalase attenuates SSL-induced Fyn kinase activity in HaCaT cells. NAC or catalase inhibits SSL-induced Fyn downstream signaling. HaCaT cells were treated with (C) NAC or (D) catalase at the indicated concentrations for 1 h and then irradiated with SSL (60 kJ/m^2) and harvested. (E) Hydrogen peroxide (H$_2$O$_2$) stimulates Fyn kinase activity in HaCaT (a) and MEFs (b). HaCaT cells and MEFs were treated with H$_2$O$_2$ (200 μM) and harvested at the indicated time points. (F) Fyn downstream signaling is

activated by H_2O_2 in Fyn$^{+/+}$ but not Fyn$^{-/-}$ MEFs. Fyn$^{+/+}$ and Fyn$^{-/-}$ MEFs were treated with H_2O_2 (200 μM) and harvested at the indicated time points. For A, B, and E, Fyn kinase activity was measured as described in Materials and Methods and for C, D, and F, Western blot analysis was performed using antibodies specific for the indicated proteins. For A, B, and E, the asterisks (**) indicate a significant ($p < 0.01$) difference compared to the untreated control and data are represented as means ± S.D. from triplicate experiments. For C, D and F, Western blots are representative of similar results from duplicate experiments.
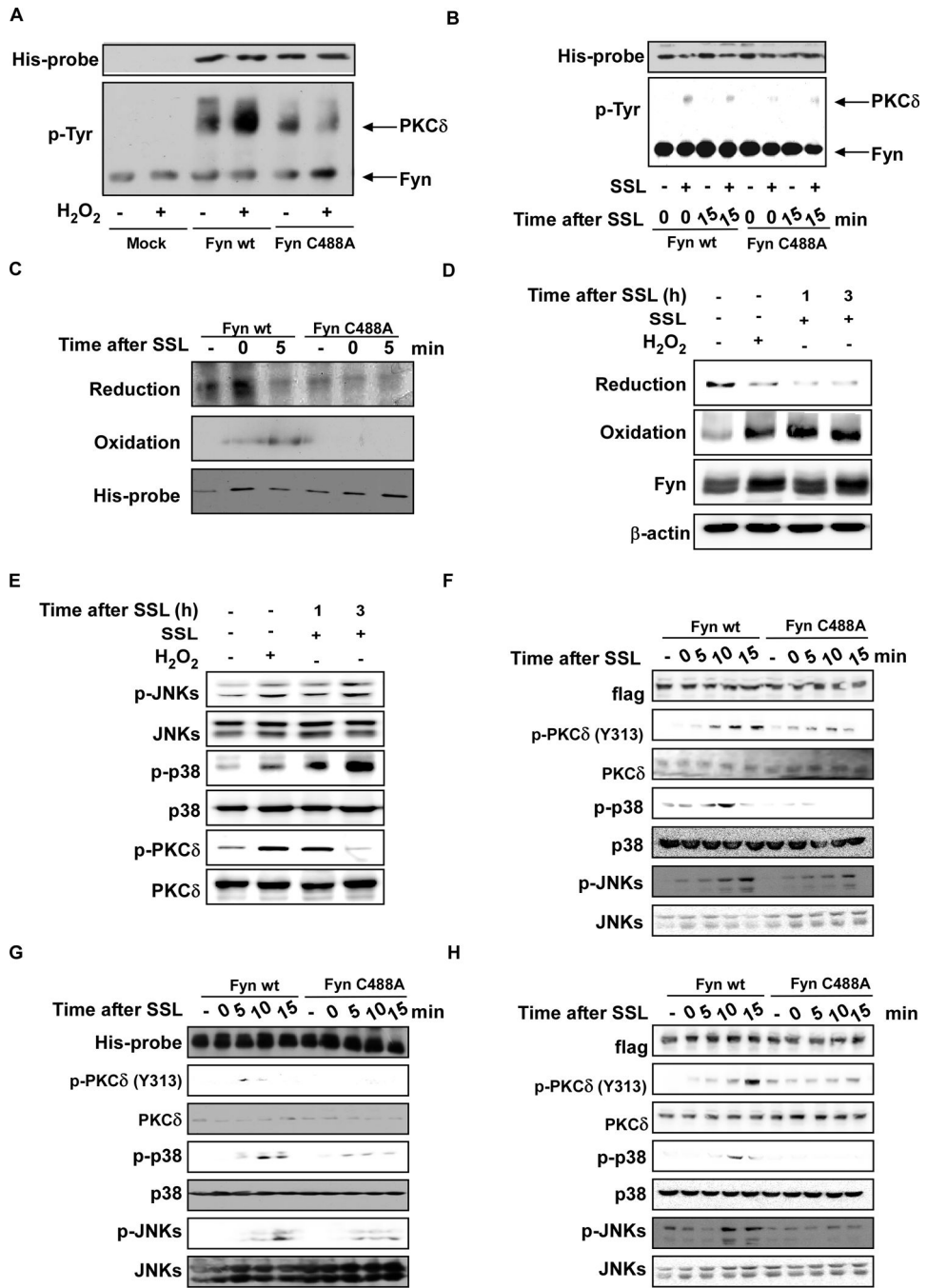
Figure 3.
ROS directly activate Fyn. (A) *In vitro* kinase assay of Mock, Fyn wildtype (wt) and mutant Fyn (C488A) proteins in the presence or absence of H_2O_2. HEK293T cells were transfected with a Mock, Fyn wt or Fyn mutant C488A vector and treated with 5 μM PP2 for 2–5 h to inactivate basal Fyn activity. Cells were disrupted in lysis buffer containing 5 μM PP2. His-tagged Fyn was immunoprecipitated at room temperature (24°C) in the presence or absence of 15 μM H_2O_2 in kinase buffer (40 μl) containing 100 μM ATP and 0.5 μg PKCδ for 45 sec with continuous mixing. Kinase activity was measured by Western blot using a

phosphotyrosine antibody. (B) *Ex vivo* kinase assay of Fyn wt and mutant Fyn C488A cells with or without exposure to SSL. HeLa cells were transfected with Fyn wt or mutant Fyn C488A and incubated for 24 h before serum starvation for 12 h. Cells were treated with SSL (60 kJ/m^2) and harvested at the indicated time points. Cells were disrupted and His-tagged Fyn was immunoprecipitated and incubated at 30°C with kinase buffer (40 μl) containing 100 μM ATP and 0.5 μg PKCδ for 15 min with continuous mixing. Kinase activity was measured by Western blot using a phosphotyrosine antibody. (C) SSL induces a change in redox status of cysteine residues in Fyn. BIAM-mediated carboxymethylation (reduction) and IAA and BIAM-mediated double carboxymethylation (oxidation) were measured as described in Methods. (D and E) SSL induces a change in redox status and downstream signaling *in vivo*. SSL (96 kJ/m^2) radiation and H$_2$O$_2$ (100 μM) were administered to SKH-1 hairless mice, which were then sacrificed at the indicated times. BIAM-mediated carboxymethylation (reduction) and IAA and BIAM-mediated double carboxymethylation (oxidation) were measured as described in Materials and Methods (D) and Signal transduction was measured by Western blotting (E). Signal transduction induced by SSL was assessed in (G) Fyn$^{-/-}$ MEFs, (F) HaCaT viral transduction with wt or mutant Fyn (C488A) and (G) HeLa cells transfected with wt or mutant Fyn (C488A). Cells were exposed to SSL and harvested at the indicated time points for Western blot analysis using specific antibodies. Western blots are representative of similar results from duplicate experiments.
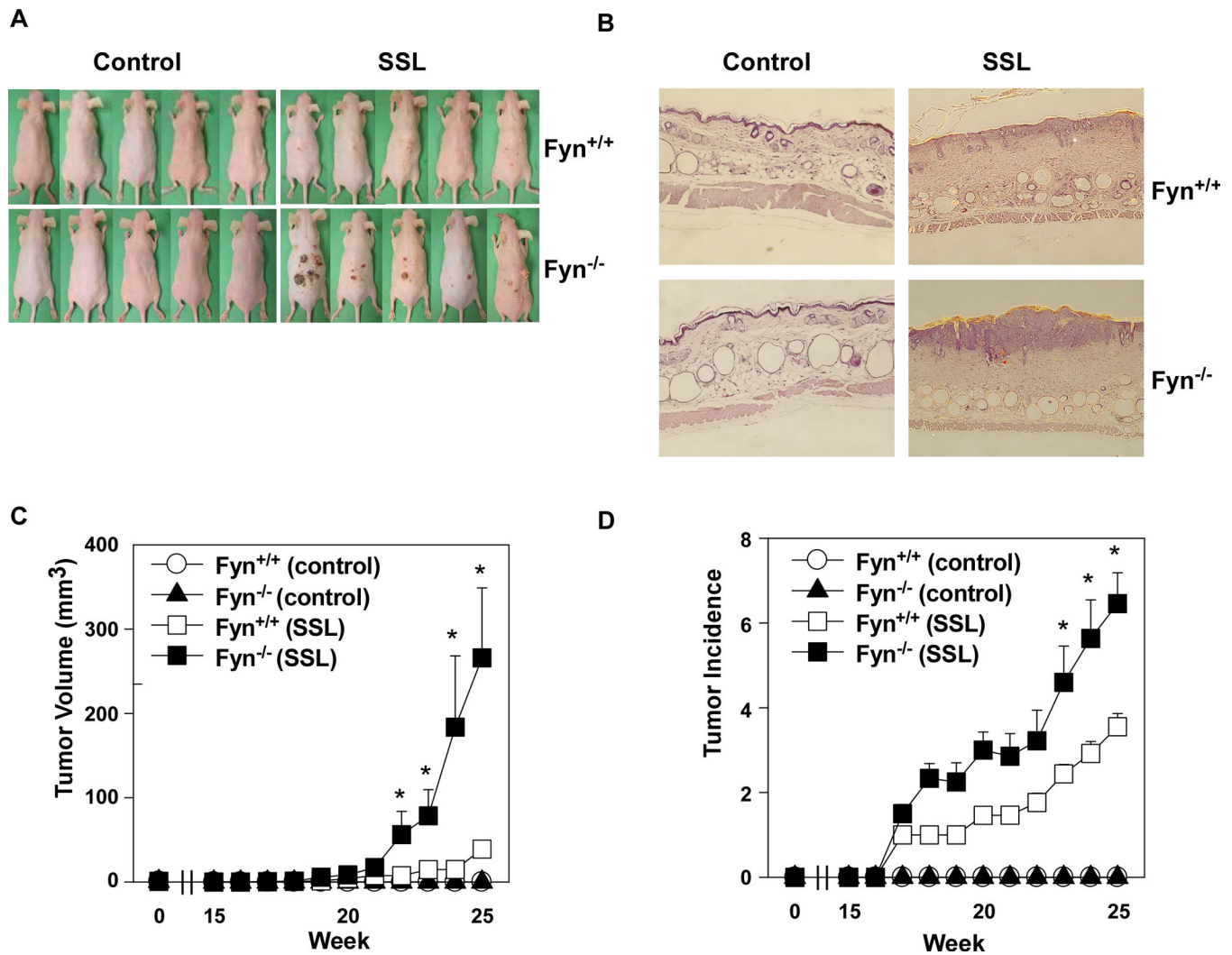
Figure 4.
Compared to wildtype mice, Fyn-deficient SKH-1 hairless mice (Fyn$^{-/-}$) develop larger and greater numbers of tumors when exposed to SSL. SKH-1 hairless Fyn wildtype (Fyn$^{+/+}$) and Fyn$^{-/-}$ mice were divided into 4 groups as follows: Group 1, no SSL Fyn$^{+/+}$; Group 2, no SSL Fyn$^{-/-}$; Group 3, SSL-treated Fyn$^{+/+}$; and Group 4, SSL-treated Fyn$^{-/-}$. The details of SSL exposure are described in Materials and Methods. (A) External appearance of tumors. (B) Skin and tumor samples were fixed in 10% NBF and processed for H&E staining. (C) Tumor volume was calculated using the formula: tumor volume (mm^3) = (length × width × height × 0.52). (D) Average number of tumors per mouse. Data are shown as means ± S.E. The asterisk indicates a significant difference (*, $p < 0.01$) between the SKH-1 Fyn$^{+/+}$ and SKH-1- Fyn$^{-/-}$ groups irradiated with SSL.
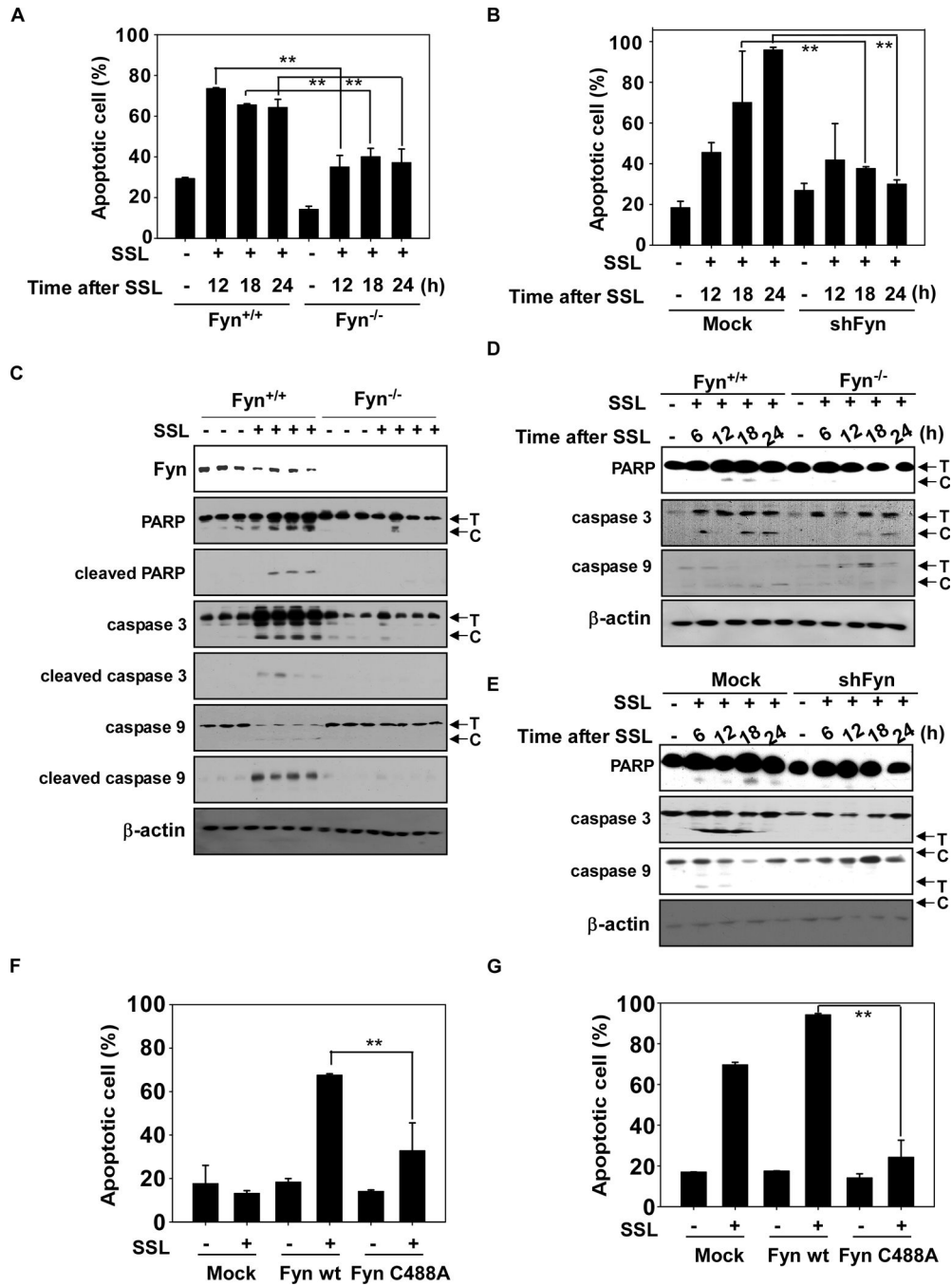
Figure 5.
Fyn deficiency confers resistance against SSL-induced apoptosis. (A) MEFs and (B) HaCaT cells deficient in Fyn are resistant to SSL-induced apoptosis. Apoptosis was determined by flow cytometry as described in Methods. SSL-induced apoptotic signaling is impaired in skin samples from Fyn$^{-/-}$ mice compared to wildtype animals (C). Fyn$^{-/-}$ MEFs (D) and shFyn HaCaT cells (E) also impaired SSL-induced apoptotic signaling compared to wt or Mock cells. Cells were exposed to SSL and harvested at the indicated time points for Western blot analysis using specific antibodies. Western blots are representative of similar

results from duplicate experiments. Fyn$^{-/-}$ MEFs (F) and HaCaT cells (G) transduced with wt or mutant Fyn (C488A). Cells were exposed to SSL and harvested at 12 h. Apoptosis was determined by flow cytometry as described in Materials and Methods. T and C indicate the total and cleaved forms, respectively. Data are shown as means ± S.D. from duplicate experiments. The asterisks (**) indicate a significant difference ($p < 0.01$) between Fyn$^{+/+}$ and Fyn$^{-/-}$ MEFs or mock-transfected and shFyn-expressing HaCaT cells.
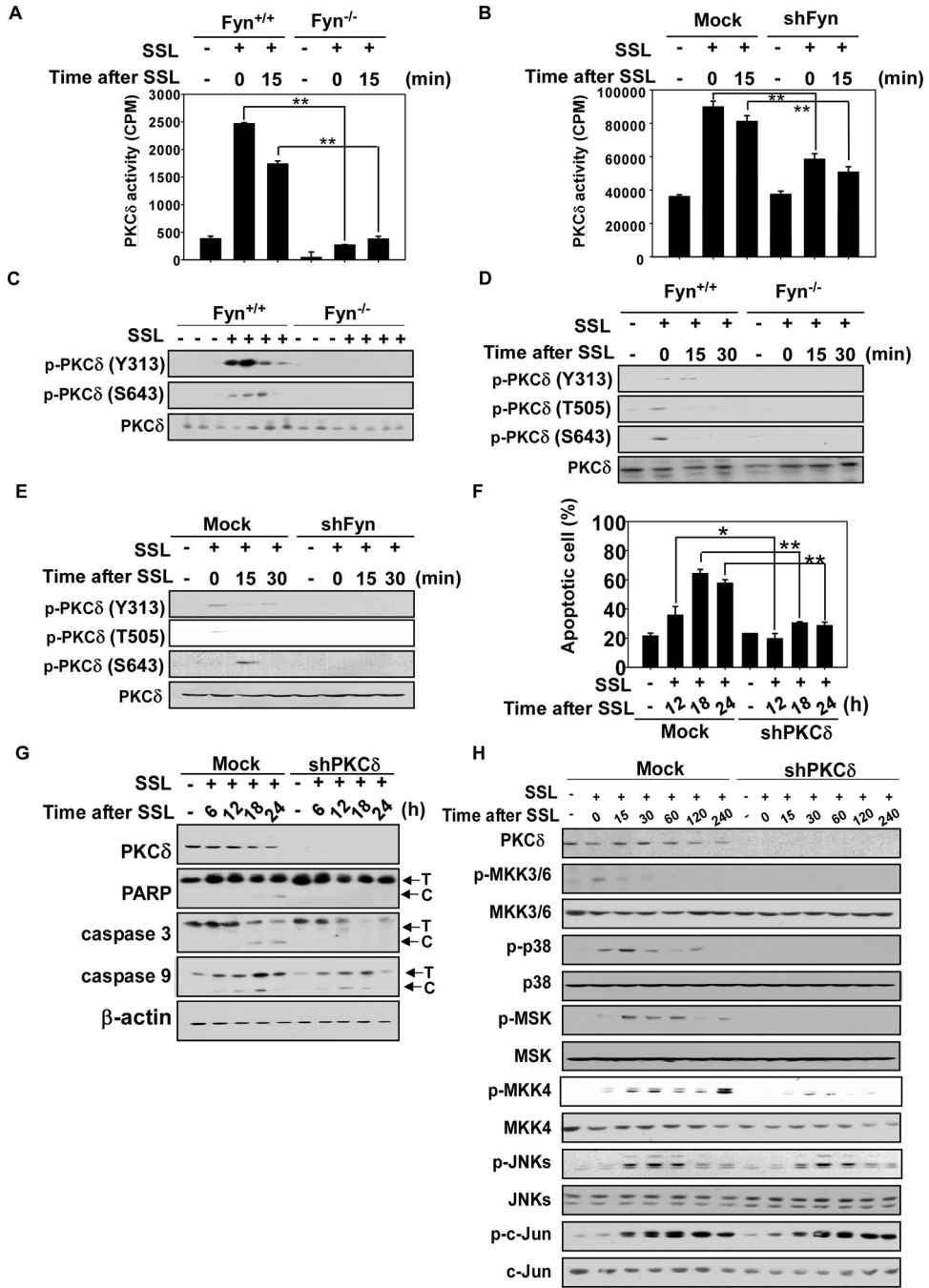
Figure 6.
Fyn deficiency inhibits SSL-induced PKCδ activity. (A and B) Fyn^{+/+} and Fyn^{−/−} MEFs (A) and mock-transfected and shFyn-expressing HaCaT cells (B) were irradiated with SSL (60 kJ/m^{2}) and harvested at the indicated time points. Cell lysates (500 μg) were incubated with protein-A/G beads (20 μL) for 1 h at 4°C. The mixture was centrifuged at 12,000 rpm for 5 min at 4°C, and a PKCδ antibody (5 μL) was added to the supernatant fraction and gently rocked overnight at 4°C. The tubes were centrifuged and pellets were washed twice. The pellets were then resuspended in 6.5 μL of kinase buffer supplemented with 10 μL of a

diluted [γ-^{32}P] ATP solution and 2.5 µL of a PKC substrate peptide (250 µM) and incubated for 30 min at 30°C. (C, D and E) Fyn knockout or deficiency inhibits SSL-induced PKCδ phosphorylation in mouse skin, MEFs and HaCaT cells. (C) Skin samples from Fyn$^{+/+}$ and Fyn$^{-/-}$ mice were harvested at 30 weeks after 12 weeks of exposure to SSL. Mouse skin was prepared as described in Materials and Methods. (D) Fyn$^{+/+}$ and Fyn$^{-/-}$ MEFs, and (E) Mock-transfected and shFyn-expressing HaCaT cells were irradiated with SSL (60 kJ/m^2) and harvested for Western blot analysis 15 min later. (F) PKCδ deficiency confers resistance against SSL-induced apoptosis. Apoptosis was determined by flow cytometry as described in Materials and Methods. (G and H) SSL-induced apoptotic signaling and PKCδ expression is impaired in shPKCδ-expressing HaCaT cells. Cells were exposed to SSL and harvested at the indicated time points. Mock-transfected and PKCδ-expressing HaCaT cells were irradiated with SSL (60 kJ/m^2) and harvested at various times as indicated. Western blot analysis was performed using specific antibodies, with representative blots shown from duplicate experiments that gave similar results. T and C indicate the total and cleaved forms, respectively. Data (A, B, F) are shown as means ± S.D. from triplicate experiments. The asterisks (*, **) indicate a significant difference ($p < 0.05$, $p < 0.01$).